Sensors and Materials, Vol. 34, No. 11 (2022) 4237–4245
MYU Tokyo

S & M 3108

Novel Self-powered Flexible Thin Bite Force Sensor with Electret and Dielectric Elastomer

Kenta Ichikawa and Wataru Hijikata*

Department of Mechanical Engineering, School of Engineering, Tokyo Institute of Technology,
2-12-1 Ookayama, Meguro-ku, Tokyo 152-8550, Japan

(Received September 28, 2022; accepted October 26, 2022)

Keywords: bite force, force sensor, self-powered mouthguard, electret, dielectric elastomer

Monitoring the bite force is valuable in the treatment of bruxism, an unconscious oral habit. Conventional bite force sensors used in clinical practice are unsuitable for wearable bite force measurement systems because of their size and measurement principles. In this study, a self-powered bite force sensor composed of an electret and a dielectric elastomer is proposed to realize a mouthguard-type wearable bite force measurement system. A theoretical model of the sensor was constructed to compensate for the nonlinearity between the applied bite force and sensor output voltage. A fabricated large-scale prototype sensor and theoretical model accurately estimated an applied force of up to 50 N. The proposed sensor is expected to realize a self-powered bite force monitoring system by making it thin and embedding it in a mouthguard.

1. Introduction

Bite force is one of the most effective indicators of oral health. Because bite force is greatly influenced by periodontal and tooth conditions, the measurement of bite force is utilized in the diagnosis of oral diseases such as periodontal disease and tooth decay. In addition, bite force is used as a surrogate index of masticatory function.(1) Nutritional intake through diet is qualitatively and quantitatively restricted when bite force decreases. Iwasaki *et al.*(2) reported that a lower maximum bite force increases the risk of developing frailty among elderly people, which is a clinical syndrome with reduced mobility and physical function, resulting in a high risk of health-related issues, including disability, hospitalization, and mortality.(3–5) Regular bite force measurements are expected to be helpful for the early detection and treatment of such problems.

The measurement of bite force can be employed in the diagnosis of bruxism. Bruxism is an unconscious oral habit that can be categorized into three types: tapping, clenching, and grinding;(6) these manifest themselves during wakefulness and sleep and generate significant bite forces that damage the teeth and jaws, causing temporomandibular disorders and dentin hypersensitivity.(7,8) There is no curative therapy for bruxism thus far; therefore, measurement of the unconscious behavior of bruxism is required for effective coping therapy.

*Corresponding author: e-mail: hijikata.w.aa@m.titech.ac.jp
https://doi.org/10.18494/SAM4134

ISSN 0914-4935

To meet the aforementioned requirements, several bite force sensor systems have been developed.[9,10] The sensor must be sufficiently thin not to interfere with occlusion to measure bite force in the maximal intercuspal position, which is the best-fit position of the opposing teeth. Furthermore, a wearable measurement system is required to monitor bruxism during sleep. In current clinical practice, a system that measures bite force based on the color change of a pressure-sensitive film and a stick-shaped sensor with a small load cell is widely used.[11] However, the pressure-sensitive film-type sensor only measures the maximum occlusal force once, and the stick-type sensor is sufficiently thick for a significant offset from the maximal intercuspal position during measurement. A thin and continuous bite force sensor is required to realize bite force measurement with intraoral wearable devices such as mouthguard-type devices.[12] Piezoelectric, piezoresistive, and capacitive force sensors have been developed as thin-film force sensors and are expected to be useful for bite force measurements.[13–15] However, these sensors require a power supply from an external power source and are unsuitable for wearable sensing systems independent of the oral cavity.

In this study, we propose a wearable bite force measurement system with a thin force sensor embedded in a mouthguard. A self-powered sensor that does not require an external power source can be realized by utilizing an electret for the sensing principle. The thin and flexible force sensor follows the shape of the occlusal surface of the mouthguard so as not to interfere with the occlusion. In this study, we validate the working principle of the proposed bite force sensor using a large-scale prototype.

2. Materials and Methods

2.1 Working principle

The proposed bite force measurement system is illustrated in Fig. 1. The bite force sensor was embedded in a double-layered mouthguard; it was fabricated by laminating an electret, dielectric elastomer, and electrodes. The thickness of the bite force sensor should be less than 200 μm so as not to interfere with occlusion. An electret is a dielectric material with a quasi-permanent charge on its surface. Opposite charges are distributed to each electrode by electrostatic induction owing to the charges held on the electret. Bite force application resulted in significant deformation of the dielectric elastomer layer. This deformation increased the electrical capacitance of the dielectric elastomer layer, which generated an induced current between the electrodes. On bite force retraction, the dielectric elastomer layer returns to its initial state owing to its restoring force, yielding a reverse-induced current. Ichikawa and Hijikata utilized this laminated structure as an energy harvester, which generated electricity from bite force, and showed that the proposed structure has a high output performance under bite force, which is 560 times higher than that of a piezoelectric element (polyvinylidene difluoride) of the same dimensions.[16] In this study, we developed a theoretical model of the proposed structure that represents the relationship between input force and output voltage. The proposed structure was utilized as a bite force sensor by solving the inverse problem of the theoretical model.

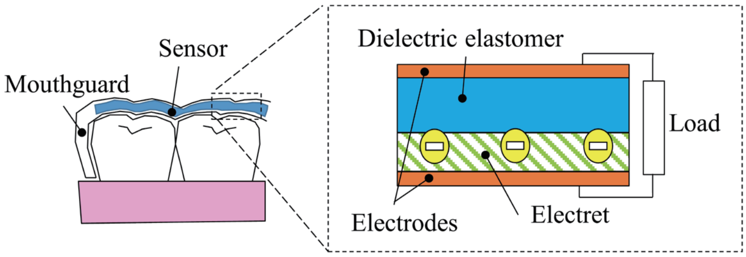

Fig. 1. (Color online) Schematic of proposed bite force measurement system.

2.2 Materials and fabrication

An amorphous fluoropolymer, CYTOP (CTL-809M, AGC Inc.), was used to fabricate the electret. To fabricate the large-scale prototype for principle validation, 10-μm-thick CYTOP was coated on a 1-mm-thick copper electrode. It was cured by heating at 100 °C for 1 h, then at 230 °C for 1 h. After curing, the fluoropolymer was treated with a corona discharge to make it an electret. The corona discharge treatment was performed for 10 min with a −9 kV wire electrode at a distance of 35 mm from the CYTOP and a −3 kV grid electrode at a distance of 17.5 mm from the CYTOP.

Silicone rubber (Dragon Skin 10 FAST, Smooth-On Inc.) was used as the dielectric elastomer. It was also coated on a 1-mm-thick copper electrode with a thickness of 100 μm.

2.3 Theoretical model of the proposed sensor

To utilize the proposed structure as a bite force sensor, a theoretical model that converts the output voltage v into an applied force f was constructed. The theoretical model consisted of two stages: a rubber elasticity model and an electrical circuit model. When bite force is applied to the sensor, the dielectric elastomer is deformed, and an induced current is generated accordingly. The rubber elasticity model represents the relationship between the bite force and elastomer deformation, whereas the electrical circuit model represents the relationship between the elastomer deformation and output voltage.

Figure 2 shows the equivalent circuit diagram of the proposed structure. The electret and dielectric elastomer layers were modeled as capacitances C_{DE} and C_{EL}, respectively. The sum of the electrical charges on both capacitances Q_{DE} and Q_{EL} equals the charge held on electret Q_0 as follows:

$$Q_{DE} + Q_{EL} = Q_0. \tag{1}$$

The output voltage v and current i are described as

$$v = \frac{Q_{DE}}{C_{DE}} - \frac{Q_{EL}}{C_{EL}} = Ri_R, \tag{2}$$

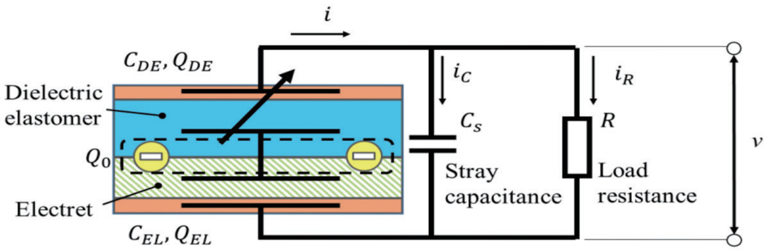

Fig. 2. (Color online) Equivalent circuit diagram of the proposed sensor.

$$i = \frac{\partial Q_{DE}}{\partial t} = i_R + i_C, \tag{3}$$

where R is the load resistance and i_R and i_C are the currents through the load resistance and stray capacitance C_S, respectively. The current through the stray capacitor can also be described as

$$i_C = C_S \frac{\partial v}{\partial t}. \tag{4}$$

Combining Eqs. (1)–(4), the circuit equation can be derived as

$$\alpha \frac{1}{C_{DE}} + \beta \frac{\partial}{\partial t}\left(\frac{1}{C_{DE}}\right) + \gamma = 0, \tag{5}$$

where coefficients α, β, and γ are derived as

$$\alpha = \frac{Q_{DE}}{R} + C_S \frac{\partial Q_{DE}}{\partial t}, \tag{6}$$

$$\beta = C_S Q_{DE}, \tag{7}$$

$$\gamma = \left(1 + \frac{C_S}{C_{EL}}\right)\frac{\partial Q_{DE}}{\partial t} + \frac{Q_0 + Q_{DE}}{RC_{EL}}. \tag{8}$$

By solving Eq. (5) numerically using the measured output voltage v, the capacitance of the dielectric elastomer C_{DE} can be obtained. From the definition of the capacitance, the elongation ratio of the dielectric elastomer λ can be obtained as

$$\lambda = \frac{\varepsilon_{DE} S}{d_{DE} C_{DE}}, \tag{9}$$

where ε_{DE}, d_{DE}, and S are the dielectric constant, equilibrium thickness, and cross-sectional area of the dielectric elastomer, respectively.

The third-order Mooney–Rivlin model was adopted as the rubber elasticity model.[17] The strain energy density function W is expressed as

$$W = \sum_{i+j=1}^{3} C_{ij} \left(I_1 - 1\right)^i \left(I_2 - 1\right)^j , \tag{10}$$

$$I_1 = \lambda^2 + 2\lambda^{-1}, \tag{11}$$

$$I \quad = 2\lambda + \lambda^{-} \quad , \tag{12}$$

where C_{ij} are material constants and I_1 and I_2 are the first and second invariants of the strain, respectively. When the boundary condition is assumed to be uniaxial compression, the force applied to the dielectric elastomer is described as

$$f = 2S\left(\lambda - \lambda^{-2}\right)\left(\frac{\partial W}{\partial I_1} + \frac{1}{\lambda}\frac{\partial W}{\partial I_2}\right). \tag{13}$$

By substituting the elongation ratio of the dielectric elastomer λ derived from the electrical circuit model into Eq. (13), the applied bite force f can be obtained.

2.4 Experimental method

A large-scale prototype was fabricated by stacking the electret and dielectric elastomer coated on the electrodes, as shown in Fig. 3(a). Compression experiments were conducted to evaluate the prototype and construct a theoretical model. The experimental apparatus is shown in Fig. 3(b). The apparatus applies a compressive load to the prototype using a cam and spring with the maximum compressive load set between 20 and 50 N by changing the spring stiffness. The applied force was measured using a load cell (LCN-A-1KN, Kyowa Electronic Instruments Co. Ltd.). The fabricated prototype was connected to a load resistor. The output voltage of the sensor (voltage drop across the load resistance) was measured using a digital oscilloscope

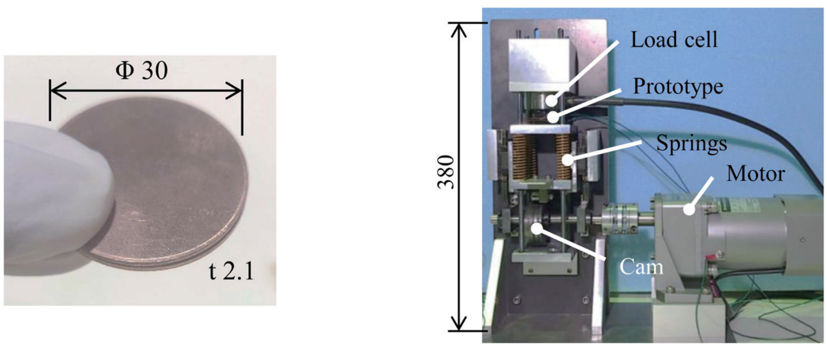

(a) (b)

Fig. 3. (Color online) (a) Photograph of fabricated prototype and (b) experimental apparatus.

(PicoScope 5442D, Pico Technologies, Inc.). A cyclic load with a frequency of 1.2 Hz was applied to simulate chewing movements to calibrate the prototype sensor, and the applied force and output voltage were simultaneously measured.

3. Results and Discussion

Figure 4 shows the output voltage and applied force data used for calibration and the force estimated by the theoretical model after calibration. Sensor calibration was conducted by optimizing the physical parameters of the theoretical model to minimize the sum of the squared errors of the estimated and measured forces by offline calculation. The calibration results of each parameter of the theoretical model are listed in Table 1.

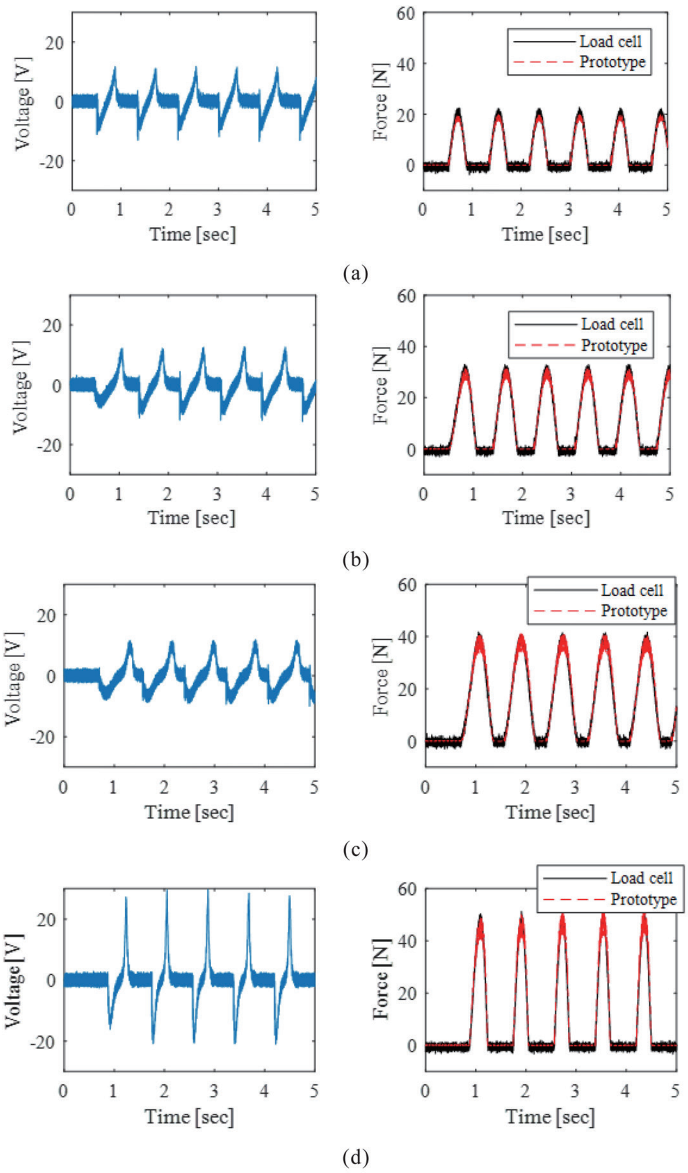

Fig. 4. (Color online) Experimental data for calibration with several maximum forces. (a) Max. 20 N. (b) Max. 30 N. (c) Max. 40 N. (d) Max. 50 N.

Table 1
Calibration results of the theoretical model.

Parameters	Unit	Values
Capacitance of electret C_{EL}	F	1.32×10^{-7}
Quasi-permanent charges on electret Q_0	C	-1.29×10^{-4}
Dielectric constant of dielectric elastomer ε_{DE}	—	8.33
Cross-sectional area of dielectric elastomer S	m^2	7.06×10^{-4}
Equilibrium thickness of dielectric elastomer d_{DE}	m	3.60×10^{-4}
Load resistance R	Ω	1.16×10^{8}
Stray capacitance C_S	F	5.30×10^{-11}
Material constant C_{10}	MPa	2.47×10^{2}
Material constant C_{01}	MPa	−92.4
Material constant C_{20}	MPa	−74.8
Material constant C_{11}	MPa	−6.09
Material constant C_{02}	MPa	13.9
Material constant C_{30}	MPa	−0.185
Material constant C_{21}	MPa	12.2
Material constant C_{12}	MPa	−8.31
Material constant C_{03}	MPa	5.89

The forces estimated by the theoretical model are in good agreement with the data measured by the load cell. The amplitude of the output voltage depends not only on the maximum compressive force but also on the frequency of the applied force. As shown in Fig. 5, the calibrated sensor and the model accurately estimated the force even under compression conditions with frequencies different from the calibration data (0.17 and 2.6 Hz, respectively). Although the actual maximum bite force is greater than that under the experimental conditions,(18) the experimental results show that the prototype has sufficient capability to detect occlusal movements. The range of the sensor depended on the elasticity of the dielectric elastomer layer. The sensor range could be extended to the expected maximum bite force by optimizing the dielectric elastomer material.

In addition, to evaluate the response speed, a step-like compression load was applied to the sensor, and its response was compared with that of the load cell, as shown in Fig. 6. The estimation of the force by the proposed sensor and model was faster than by the load cell attached to the experimental apparatus with a natural frequency of 5.3 kHz. As the response speed of a load cell is considered to be approximately one-tenth of its natural frequency, the proposed sensor was demonstrated to have a higher response speed than that of the load cell.

To embed the sensor into the mouthguard, a thin and flexible sensor sheet with a thickness of less than 200 μm should be fabricated. The fabricated prototype was thick and noncompliant for embedding into the mouthguard because of the 1-mm-thick copper electrode. These electrodes are also used as the substrate for electret and dielectric elastomer. The improved fabrication process is required to fabricate electrets and dielectric elastomers using thin and low-strength electrodes. In our previous work,(16) electrets and elastomers were fabricated on a 10-μm-thick copper electrode to compose an energy harvester. These components were sufficiently thin and flexible for embedding in the mouthguard. A thin and flexible sensor sheet based on the proposed principle can potentially be fabricated using the same fabrication method.

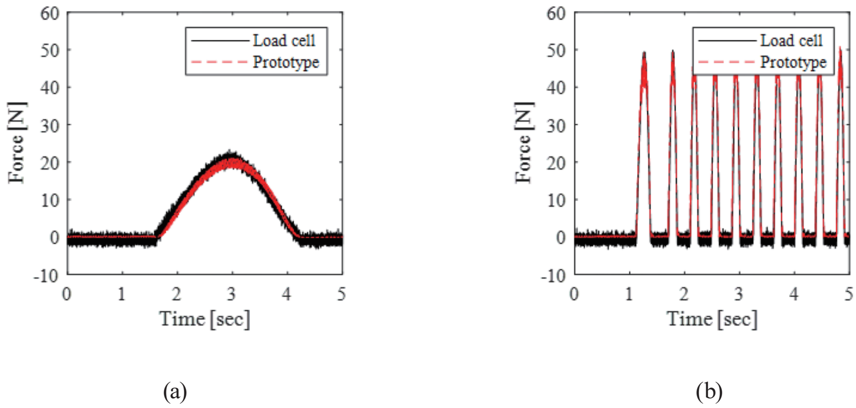

Fig. 5. (Color online) Estimation results obtained by the model under different compression conditions. (a) Low frequency (0.17 Hz). (b) High frequency (2.6 Hz).

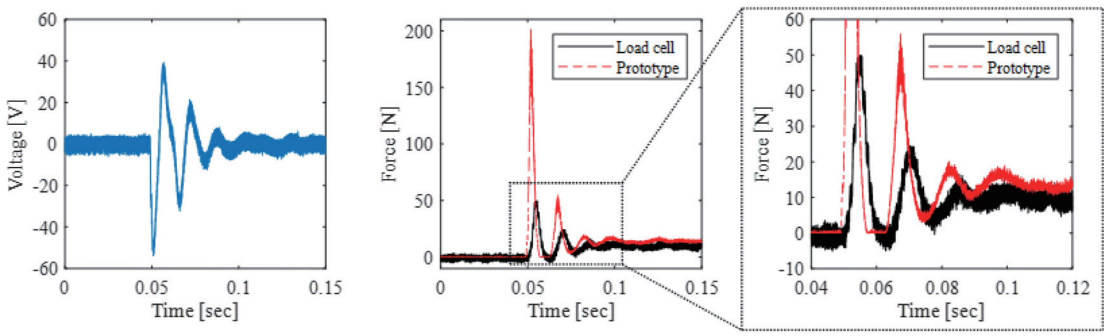

Fig. 6. (Color online) Experimental and estimation results under step-like force input.

The proposed sensing principle was demonstrated to be capable of force sensing without an external power source by utilizing an electret that holds a quasi-permanent electrical charge. It is necessary to sense without an external power source and to process and communicate the measurement data to realize a mouthguard-type wearable bite force measurement system. The proposed electret and dielectric elastomer structure can also function as an energy harvester. In our previous experiments,[16] the proposed structure generated sufficient power to transmit four bytes of data once every 5 min under a load equivalent to chewing movement. A self-powered bite force measurement system can be realized by integrating functions such as a bite force sensor and an energy harvester.

4. Conclusions

In this study, a novel bite force sensor consisting of an electret and dielectric elastomer was proposed. The proposed sensor could generate an electrical signal from force input without an external power source via electrostatic induction. A theoretical model of the sensor was also constructed to compensate for the nonlinearity between the applied force and the output voltage. Experiments using a large-scale prototype sensor demonstrated that the proposed sensor and theoretical model accurately estimated forces up to 50 N. Furthermore, it was also revealed that the proposed sensor has a high response speed. The development of a thinner sensor and improvement of the range of sensors will be conducted in future work to realize a mouthguard-type wearable bite force measurement system.

Acknowledgments

This work was supported by JSPS KAKENHI Grant Number 21J13262.

References

1 X. Wang, G. Zheng, M. Su, Y. Chen, H. Xie, W. Han, Q. Yang, J. Sun, and J. Chen: Food Sci. Hum. Wellness **8** (2019) 149. https://doi.org/10.1016/j.fshw.2019.03.009
2 M. Iwasaki, A. Yoshihara, N. Sato, M. Sato, K. Minagawa, M. Shimada, M. Nishimuta, T. Ansai, Y. Yoshitake, T. Ono, and H. Miyazaki: J. Oral Rehabil. **45** (2018) 17. https://doi.org/10.1111/joor.12578
3 Q-L. Xue: Clin. Geriatr. Med. **27** (2011) 1. https://doi.org/10.1016/j.cger.2010.08.009
4 H. Miura, S. Watanabe, E. Isogai, and K. Miura: J. Oral Rehabil. **28** (2001) 592. https://doi.org/10.1046/j.1365-2842.2001.00716.x
5 FF. Hakeem, E. Bernabé, and W. Sabbah: Gerodontology **36** (2019) 205. https://doi.org/10.1111/ger.12406
6 G. Demjaha, B. Kapusevska, and B. Pejkovska-Shahpaska: Open Access Maced. J. Med. Sci. **7** (2019) 876. https://doi.org/10.3889/oamjms.2019.196
7 H. von Piekartz, C. Rösner, A. Batz, T. Hall, and N. Ballenberger: Musculoskelet. Sci. Pract. **45** (2020) 102073. https://doi.org/10.1016/j.msksp.2019.102073
8 T. Scaramucci, TE. de Almeida Anfe, S. da Saliva Ferreira, AC. Frias, and MA. Sobral: Clin. Oral Investig. **18** (2014) 651. https://doi.org/10.1007/s00784-013-1008-1
9 R. Shigemitsu, N. Yoda, T. Ogawa, T. Kawata, Y. Gunji, Y. Yamakawa, K. Ikeda, and K. Sasaki: Comput. Biol. Med. **54** (2014) 44. http://dx.doi.org/10.1016/j.compbiomed.2014.08.018
10 D. Zhang, X. Han, Z. Zhang, J. Liu, C. Jiang, N. Yoda, X. Meng, and Q. Li: Int. J. Numer. Methods Biomed. Eng. **33** (2017) e2889. https://doi.org/10.1002/cnm.2889
11 Y. Gu, Y. Bai, and X. Xie: Front. Bioeng. Biotechnol. **9** (2021) 665081. https://doi.org/10.3389/fbioe.2021.665081
12 T. Arakawa, K. Tomoto, H. Nitta, K. Toma, S. Takeuchi, T. Sekita, S. Minakuchi, and K. Mitsubayashi: Anal. Chem. **92** (2020) 12201. https://doi.org/10.1021/acs.analchem.0c01201
13 Y. Zhu, S. Jiang, Y. Xiao, J. Yu, L. Sun, and W. Zhang: J. Mater. Sci. Mater. **29** (2018) 19380. https://doi.org/10.1007/s10854-018-0111-0
14 S. Cheng, B. Chen, Y. Zhou, M. Xu, and Z. Suo: Extreme Mech. Lett. **34** (2020) 100592. https://doi.org/10.1016/j.eml.2019.100592
15 DTW. Lin, K-D. Li, P-C. Chen, and J-Y. Kuo: Sens. Mater. **33** (2021) 3603. https://doi.org/10.18494/SAM.2021.3623
16 K. Ichikawa and W. Hijikata: Nano Energy **99** (2022) 107357. https://doi.org/10.1016/j.nanoen.2022.107357
17 C. Liu, CM. Cady, ML. Lovato, and EB. Orler: J. Mater. Sci. **50** (2015) 1401. https://doi.org/10.1007/s10853-014-8700-7
18 H. Kumagai, T. Suzuki, T. Hamada, P. Sondang, M. Fujitani, and H. Nikawa: J. Oral Rehabil. **26** (1999) 932. https://doi.org/10.1046/j.1365-2842.1999.00473.x